

## Expansion Energy and Hydration Products of Expansive Mortar at Different Temperatures

Mitsuo Ozawa<sup>1</sup>, Kentaro Suhara<sup>2</sup> and Hiroaki Morimoto<sup>3</sup>

<sup>1</sup>*Gunma University, Division of Environmental Engineering Science, Japan*

<sup>2</sup>*Denki Kagaku Kogyo K. K., Inorganic Materials Research Laboratory, Japan*

<sup>3</sup>*Gifu University, Department of Civil Engineering, Japan*

<sup>1</sup>*1-5-1, Tenjin-cho, Kiryu City, Gunma 376-8515, ozawa@gunma-u.ac.jp*

<sup>2</sup>*2209, Omi, Itoigawa-shi, Niigata 949-0393, Japan, kentaro-suhara@denka.co.jp*

<sup>3</sup>*1-1, Yanagido, Gifu City, Gifu 501-1193, morimt@gifu-u.ac.jp*

### ABSTRACT

Expansive concrete is used in construction work as an efficient way to prevent cracking and improve structural behavior. Based on the formation of ettringite and calcium hydroxide, considerable expansion of concrete at an early age can be expected. However, no universal agreement has yet been established concerning the fundamental mechanism behind effective expansive strain in concrete with curing at different temperatures. This study was conducted to clarify the expansive energy and hydration products of expansive mortar at 20, 30 and 50°C under restraint testing conditions. The results showed that the maximum values of expansive energy were  $0.75 \times 10^{-4}$  Nmm/mm<sup>3</sup> with curing at 20°C,  $1.1 \times 10^{-4}$  Nmm/mm<sup>3</sup> at 30°C and  $0.9 \times 10^{-4}$  Nmm/mm<sup>3</sup> at 50°C. The formation of ettringite (AFt) was observed in all temperature conditions using differential scanning calorimetry (DSC) and scanning electron microscopy (SEM).

**Keywords:** expansive mortar, temperature dependency, hydration products, SEM, thermal analysis

### INTRODUCTION

Expansive concrete is generally used in construction work as an efficient way to prevent cracking and improve structural behavior. Based on the formation of ettringite and calcium hydroxide, considerable expansion of concrete at an early age can be expected. With such expansive materials, either shrinkage-compensating or chemically pre-stressed types may be applied depending on the amount of expansive energy involved. As the expansive agent is activated by hydration, expansion performance may differ with curing temperatures.

In previous related work, methods based on the fundamental rule of constant expansive energy were proposed by Okamura (1974, 1978) and Tsuji (1988), while Morioka (1998) reported on the hydration reaction of a CSA-type expansive additive. Mitani (2003) investigated the restraint stress of expansive concrete under conditions of mass curing temperature hysteresis, and Kobayashi (2011) discussed the expansion properties and

hydration products of expansive mortar. Sahamitmongkol (2011) reported on the tensile behavior of restrained expansive mortar, and Khoshnazar (2012) investigated the mechanisms responsible for volume stability in calcium sulfo-aluminate phases.

However, no universal agreement has yet been established concerning the temperature dependence of expansive strain with curing at different temperatures. This paper discusses expansive energy and hydration products of expansive mortar cured at 20, 30 and 50°C as observed under restraint testing conditions.

## EXPERIMENT OUTLINE

**Restraint testing.** Tables 1 and 2 show the mixture proportions of the plain mortar (PL-M), expansive mortar (EX-M) and other materials used in this study. Ordinary portland cement was used with CSA (calcium sulfoaluminate) expansive material added at a concentration of 50 kg/m<sup>3</sup>. Tables 3 and 4 show the chemical compositions of the Portland cement and the expansive additive. Tables 5 and 6 show the material properties of the fresh concrete and the results of related compressive strength testing at 20°C, and Figure 1 shows the shapes and dimensions of the restraint specimens, which were square columns with dimensions of 75 × 75 × 254 mm as per the ASTM standard. The specimens had an invar steel bar (thermal expansion coefficient: 0.1 μ/°C) with a diameter of 10 mm at the center of the cross section, and both ends were restrained using steel plates with dimensions of 75 × 75 × 20 mm. Strain gauges were placed at the lengthwise center of the invar steel bars, and a Teflon sheet was placed between the specimen and the steel form to reduce friction. The specimen temperature and deformation caused by volume changes were monitored. After the mortar was cast in a steel form, the restrained and free specimens were both placed in a constant-temperature and constant-humidity environment (temperature: 20 ± 2°C; humidity: 60% ± 5%). After the mortar setting test (JIS A 1147) was complete, the ambient temperature was increased from 20 to 30 and then to 50°C at a rate of 1.67°C/hour as per the procedure for mass concrete. The strain of the steel bars and the temperature inside the concrete were monitored for seven days from the initial setting time.

Table 1. Mixture proportion of mortar

Type	Water-Binder	Unit weight(kg/m <sup>3</sup> )				Air	Admixture(cc/m <sup>3</sup> )	
	W/B(%)	Water	Cement	Expansive Additive	Fine aggregates	(%)	AE and Water Reducing Agent	Anti-foaming Agent
PL-M	40	258	645	—	1286	5	1475	35.4
EX-M			595	50	1283			

Table 2. Materials

Material	Material Property
Cement	Ordinary Portland Cement, Density 3.15g/cm <sup>3</sup>
Expansive Additive	CSA (Calcium sulfoaluminate), Density 2.93g/cm <sup>3</sup>
Fine Aggregate	ISO Sand, Density 2.64g/cm <sup>3</sup>
AE and Water Reducing Agent	Lignin sulfonate compound and Polyol, Density 1.23-1.27g/cm <sup>3</sup>
Anti-foaming Agent	Polyalkylene glycol, Density 0.98~1.02g/cm <sup>3</sup>

Table 3. Chemical composition of Ordinary Portland Cement

SiO <sub>2</sub>	Fe <sub>2</sub> O <sub>3</sub>	Al <sub>2</sub> O <sub>3</sub>	CaO	SO <sub>3</sub>	MgO	Igloss
20.3	2.7	4.9	64.6	3.2	1.5	1.06

Table 4. Chemical composition of Expansive Additive

SiO <sub>2</sub>	FeO <sub>3</sub>	Al <sub>2</sub> O <sub>3</sub>	CaO	SO <sub>3</sub>	f-CaO
1.5	0.5	16.1	52.8	27.5	19

Table 5. Fresh properties

Setting Temperature(°C)	20	30	50
Mortar Flow (mm)	172	176	183
Temperature of mixed mortar (°C)	22.3	20.9	20.2

Table 6. Compressive strength at 20°C

day	Compressive strength MPa	
	PL-M	EX-M
1	11.3	8.73
3	11.0	9.78
7	13.0	14.5

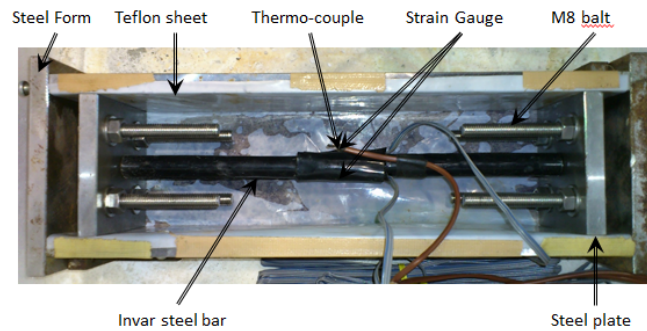


Figure 1. Specimen

Table 7. Mixture proportion of cement paste

Type	W/B (%)	Unit weight(kg/m <sup>3</sup> )		
		Water	Cement	Expansive Additive
PL-P	40	558	1395	—
EX-P			1352	42

**Differential scanning calorimetric (DSC).** Table 7 shows the mixture proportions of the plain paste (PLP) and expansive paste (EXP) used in the study. Fresh cement paste samples were cast in ziplock-type plastic bags with the temperature and relative humidity (RH) maintained at 20°C and 100% until the time of testing. Before DSC analysis was carried out, the hydration reactions were stopped at ages of 0, 0.3, 1 and 7 days via acetone immersion and vacuum drying in order to remove free water in the specimens. The samples were then finely ground and stored in sealed glass vials.

DSC was conducted using a computer-controlled furnace to heat a pair of measuring heads (one containing approximately 50 mg of the test specimen and the other as a reference cell)

in a dynamic nitrogen atmosphere. Each specimen was heated at a rate of 5°C/min. from 20 to 200°C, and then at 10°C/min. to a maximum temperature of 600°C.

The DSC heat flow signal was integrated over time to determine the quantity of heat change for each region of the curve representing a major phase in the cement paste system, and the rate of hydration production was calculated based on the quantity of heat. The peak temperatures were used to identify the major hydration products (Ramachandran 2003) with a focus on ettringite (AFt) and calcium hydroxide (Ca (OH)<sub>2</sub>).

**SEM observation.** The microstructural characteristics of the selected mortar samples (see Table 1) were determined via scanning electron microscope (SEM) observation carried out on both fractured and polished sections. Before this observation was carried out, the hydration reactions were stopped at ages of 0, 0.3, 1 and 7 days using acetone immersion and vacuum drying in order to remove free water in the specimens.

**Calculation of expansive energy.** Based on the work conservation law (Japan Concrete Institute 2003), the work of expansive concrete per unit volume was calculated from the results of unconfined restraint testing using Equations (1) and (2) below.

$$\varepsilon_{EX} = \varepsilon_{(EX\_M)} - \varepsilon_{(PL\_M)} \quad (1)$$

$$e_{che} = p \times E_s \times (\varepsilon_{EX})^2 / 2 \quad (2)$$

Here,  $\varepsilon_{EX}$  is the effective expansive strain of a steel bar,  $\varepsilon_{EX\_M}$  is the steel bar strain from expansive mortar,  $\varepsilon_{EX\_PL}$  is the steel bar strain from plain mortar,  $e_{che}$  is the value of work (N mm/mm<sup>3</sup>),  $p$  is the steel ratio (%) and  $E_s$  is the steel bar elastic modulus (N/mm<sup>2</sup>).

In this study, the value of work was considered to approximately represent the expansive energy of the mortar.

## RESULTS AND DISCUSSION

**Temporal changes in internal temperature.** Figure 2 shows temporal changes in temperature after initial setting. For the 20°C specimen, the internal temperature was around 20°C. For the 30°C specimen, the temperature reached 33°C during the 6-hour period after ambient temperature control was initiated. 12 hours after ambient temperature control was initiated, the temperature was around 30°C. For the 50°C specimen, the temperature reached 52°C during the 8-hour period after ambient temperature control was initiated. Six hours later, the temperature was around 50 ± 3°C. It was observed that the temperature inside the specimens could be controlled.

**Setting tests.** Figure 3 shows the results of the setting tests. The initial setting was from 5.6 to 7.6 hours, and the final setting was from 8.3 to 9 hours.

**Temporal changes in steel bar strain.** Figure 4 shows temporal changes in steel bar strain after initial setting for the different temperatures applied. In each expansive mortar specimen, strain values increased with expansion very rapidly during the first day and reached near-maximum levels of 250, 163 and 60 μ at 7 days for 20, 30 and 50°C, respectively. In each plain mortar specimen, strain increased with shrinkage and reached near-maximum levels of -30, -158 and -228 μ at 7 days for 20, 30 and 50°C, respectively.

**Effective expansion strain.** Figure 5 shows temporal changes in the effective expansion strain of steel bars after initial setting for the different temperatures applied. Values were calculated using Eq. (1) based on the measurement values shown in Figure 4. For each temperature, effective expansion strain increased very rapidly during the first day and reached near-maximum levels of 268, 320 and 290 μ at 7 days for 20, 30 and 50°C, respectively. No significant changes were observed between 1 and 7 days.

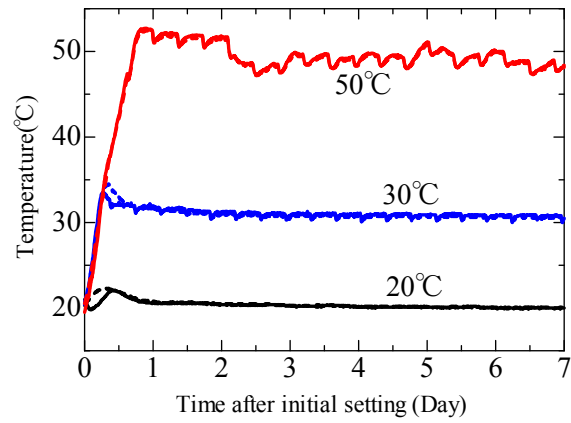


Figure 2. Temporal changes in temperature after initial setting (Mortar)

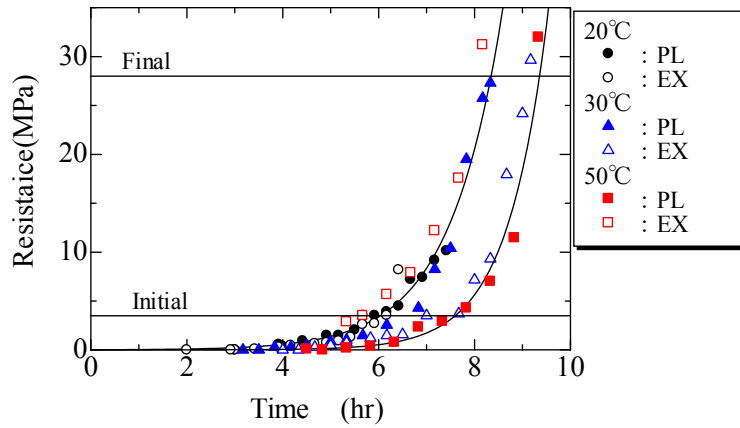


Figure 3. Setting tests (Mortar)

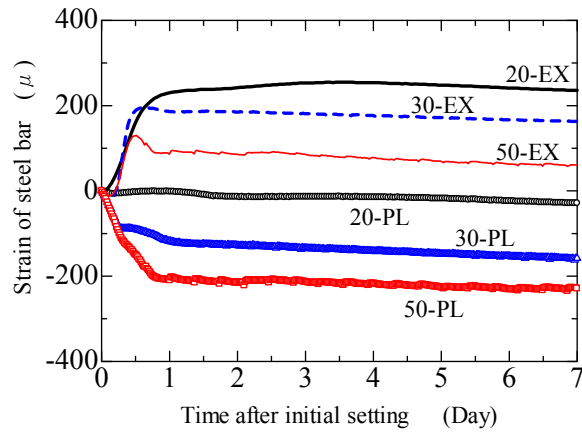


Figure 4. Temporal changes in steel bar strain after initial setting (Mortar)

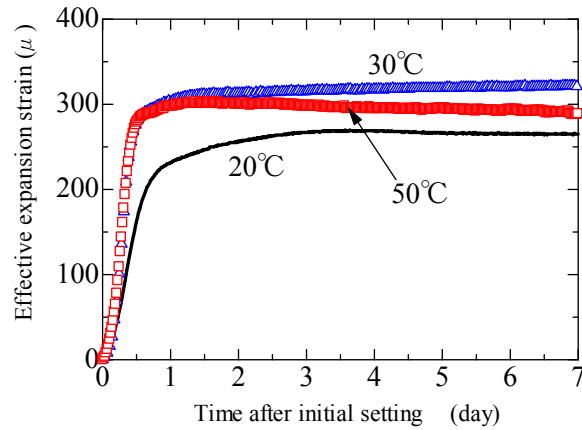


Figure 5. Temporal changes in the effective expansion strain of steel bars after initial setting (Mortar)

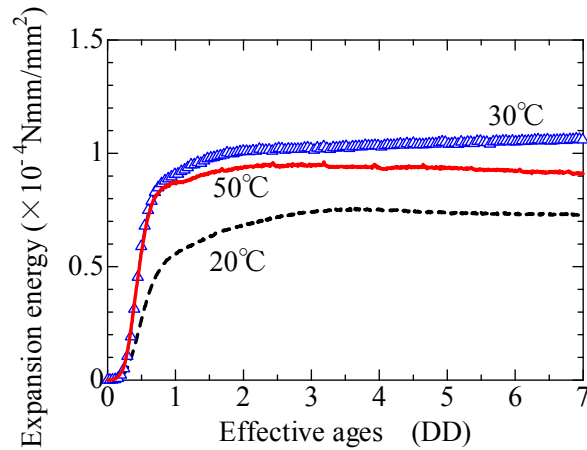


Figure 6. Expansive energy vs. effective age (Mortar)

**Expansive energy.** Figure 6 shows expansive energy vs. effective age as an indicator of maturity. Expansive energy was calculated using Eq. (2). For each temperature, expansive energy increased very rapidly during the first day and reached near-maximum levels of  $0.75 \times 10^{-4}$ ,  $1.1 \times 10^{-4}$  and  $0.9 \times 10^{-4}$  ( $\text{N} \cdot \text{mm}/\text{mm}^3$ ) at 7 days for 20, 30 and 50°C, respectively. The rates of expansive energy change for 30 and 50°C were higher than for 20°C because activation energy was provided.

**DSC results.** Figure 7 shows the relationship between production amounts of calcium hydroxide ( $\text{Ca}(\text{OH})_2$ ) (and below, CH) and the time after initial setting for 20, 30 and 50°C. For each temperature, CH amounts increased very rapidly during the first day and reached near-maximum values of 6.5, 16 and 14% at 7 days for 20, 30 and 50°C, respectively. No significant differences were observed in the cases with and without expansive additive.

Figure 8 shows the relationship between production amounts of ettringite (and below, AFt) and the time after initial setting for 20, 30 and 50°C. For 20°C, AFt amounts increased from 0.3 to 1.0 days and reached maximum values of 13 and 10% at 1 day in the cases with and without expansive additive, respectively. After 1.0 days, AFt amounts decreased to 8.3 and 6.3% for the cases with and without expansive additive, respectively. For 30°C, the AFt

amount at the initial setting time and the maximum value were 7.2 and 6.7% at 0.3 days for the cases with and without expansive additive, respectively. After 0.3 days, AFt amounts decreased and were 2.2 and 4.3% at 7 days for the cases with and without expansive additive, respectively. For 50°C, the AFt amount at the initial setting time and the maximum value were 5.3 and 5.8% at 0.3 days for the cases with and without expansive additive, respectively. After 0.3 days, AFt amounts decreased and were 2.4 and 3.9% at 1 day for the cases with and without expansive additive, respectively. After 1.0 days, no AFt was detected. It was supposed that the AFt had changed to monosulfate (and below, AFm) due to the use of gypsum at 50°C. It can therefore be inferred that AFt formation is dependent on temperature history.

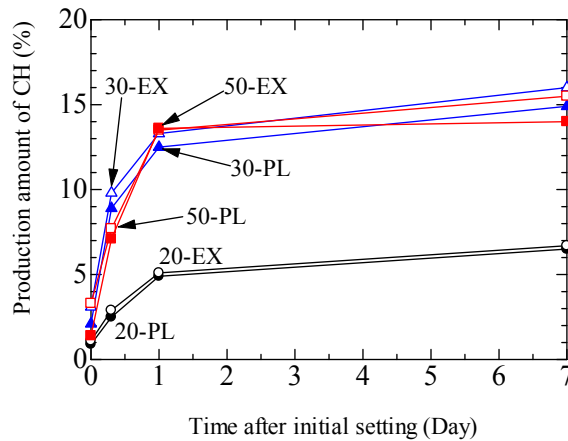


Figure 7. Production amount of CH and time after initial setting (Paste)

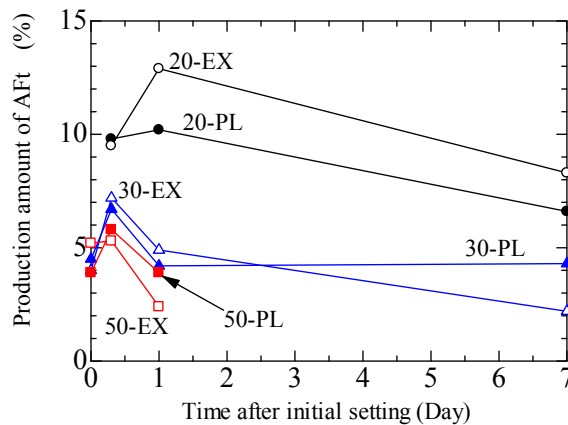


Figure 8. Production amount of AFt and time after initial setting (Paste)

**SEM observation.** Figures 9 to 11 show the results of SEM observation for expansive mortar at 0, 0.3, 1 and 7 days after initial setting for 20, 30 and 50°C. Needle crystals of AFt were observed at 7 days for 20°C and at 1 day for 30 and 50°C.

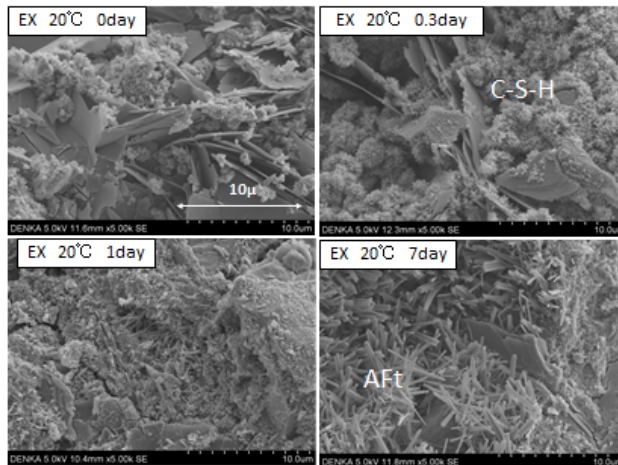


Figure 9. SEM observation (20°C)

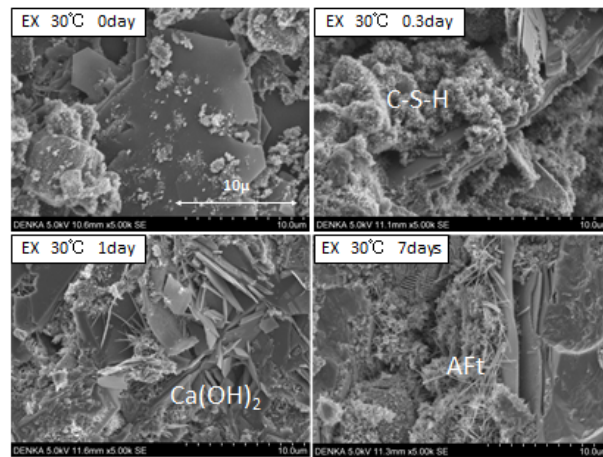


Figure 10. SEM observation (30°C)

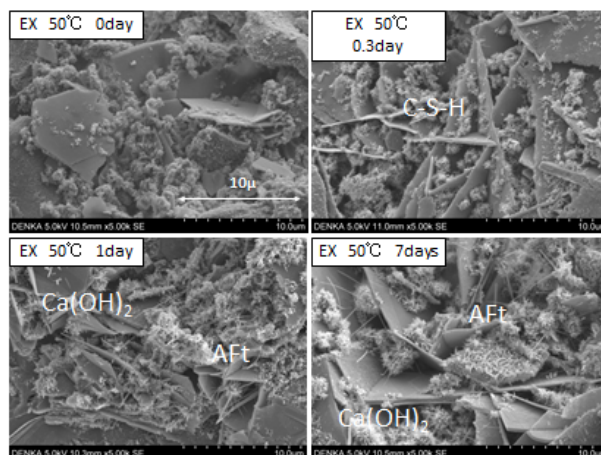


Figure 11. SEM observation (50°C)

## CONCLUSION

This paper highlights the relationship between expansive energy and hydration products of expansive mortar cured at 20, 30 and 50°C under restraint testing conditions. The main conclusions can be summarized as follows:

- 1) Expansive energy increased very rapidly during the first day. The range of maximum expansive energy was from  $0.75 \times 10^{-4}$  to  $1.1 \times 10^{-4}$  (N · mm/mm<sup>3</sup>) at 7 days for 20 to 50°C. The rates of expansive energy for 30 and 50°C were larger than that for 20°C.
- 2) CH amounts increased very rapidly during the first day. No significant differences were observed in the cases with and without expansive additive.
- 3) AFt needle crystals were observed at 7 days for 20°C and at 1 day for 30 and 50°C. From DSC results and SEM observation, it was supposed that AFt changed to AFm at 50°C.
- 4) It can be inferred that AFt formation is dependent on temperature history.

More research is required to clarify the relationship between expansive energy and hydration products of expansive concrete.

## ACKNOWLEDGEMENT

This study was supported by a 2011 grant from the Japan Cement Association. The authors are grateful to the organization for its financial support. The DSC and SEM observation support received from Mr. A. Nanasawa at Denka Co., Ltd. is also gratefully acknowledged.

## REFERENCES

- ASTM: Standard Test “Method for Restrained Expansion of Shrinkage Compensating Concrete,” C878/C878M-09.
- Japan Concrete Institute (2003) “Proceedings of JCI Symposium on Expansive Concrete for High Performance Durable Structures” (in Japanese).
- JIS A 1147 (2007) “Method of Test for Time of Setting of Concrete Mixtures by Penetration Resistance.”
- Kobayashi, S. et al. (2011) “Expansion Properties and Hydration Products of Expansive Mortar at Different Temperatures,” *J Cement and Concrete* No. 65, 95 – 102 (in Japanese).
- Khoshnazar, R., Beaudoin, J. J., Alizadeh, R. and Raki, L. (2012) “Volume Stability of Calcium Sulfoaluminate Phases,” *J Am Ceram Soc*, 1 – 6.
- Mitani, Y., Tanimura, M., Sakuma, T. and Satake, S. (2003) “Evaluation Method for Restraint Stress of Expansive Concrete under Mass Curing Temperature Hysteresis,” *Proc of JCI Symposium on Expansive Concrete for High Performance Durable Structures*, JCI, 44 – 49 (in Japanese).
- Morioka, M. (1998) “Hydration Reaction of a Calciumsulphoaluminate-type Expansive Additive,” *Proceedings of Cement & Concrete*, JCA, No. 52, 2 – 7 (in Japanese).
- Okamura, H. (1974) “Physical properties of chemically prestressed concrete,” *J JSCE*, 226, 101 – 108.

- Okamura, H., Tsuji, Y. and Maruyama, K. (1978) "Application of expansive concrete in structural elements," J Faculty Eng Univ Tokyo (B), 34 (3), 481 – 507.
- Ramachandran, V. S., Paroli, R. M., Beaudoin, J. J. and Delgado, A. H. (2003) "Handbook of Thermal Analysis of Construction Materials," William Andrew Publishing.
- Sahamitmongkol, R., Kishi, T. (2011) "Tensile behavior of restrained expansive mortar and concrete," Cement & Concrete Composites 33, 131 – 141.
- Tsuji, Y. (1988) "Estimation of Expansive Energy in Concrete Engineering," Concrete Journal, Vol. 26, No. 10, 5 – 13 (in Japanese).